# Adaptive Optimization of an Iterative Multiuser Detector for Turbo-Coded CDMA

David P. Shepherd, Fredrik Brännström, Frank Schreckenbach, Zhenning Shi, and Mark C. Reed

***Abstract*—Extrinsic information transfer (EXIT) charts are utilized to optimize the iterative multiuser detector receiver in a multiuser turbo-coded CDMA system. The (receive) power levels are optimized for the system load using a constrained nonlinear optimization approach. The optimal decoding schedule is derived dynamically using the power optimized EXIT chart and a Viterbi search algorithm. Dynamic scheduling is shown to be a more flexible approach which results in a more stable QoS for a typical system configuration than one-shot scheduling, and large complexity savings over a receiver without scheduling.**

**We verify through simulations that complexity savings of over 50% and power savings of over 8dB can be achieved. We show that the optimized power levels combined with adaptive scheduling allows for efficient utilization of receiver resources for heavily loaded systems.**

***Index Terms*—Multiuser detection, transmission technology, CDMA, wireless access, source/channel coding, transmission technology.**

## I. Introduction

In RECENT years there has been much interest in multiuser cellular systems and receiver design for coded code division multiple access (CDMA) systems has become an important field of research. Predicting the performance of a CDMA system with iterative decoding is computationally demanding even for a small number of users. Extrinsic information transfer (EXIT) chart analysis has been successfully used for describing and visualizing the convergence behavior without the need for computationally demanding simulations.

It was shown in [1] and [2] that a cellular multi-access system is more efficient when the user transmit power distribution is not uniform. Caire *et al* used linear programming and large-scale Density Evolution (DE) to optimize the power levels in a CDMA system in [3] and [1]. We propose the use of EXIT charts to optimize the power distribution. The main difference between the two approaches is the parameter used to characterize the decoding trajectory, EXIT charts using mutual information (MI) rather than density (SNR). The principle is the same - minimize the power under the constraint that successful decoding is possible. EXIT chart analysis is, however, generally considered to be more accurate than variance transfer methods for predicting convergence behavior [4]. The EXIT chart approach is also convenient as we use the resulting transfer chart for optimizing the decoding schedule.

In [5] and [6] the authors showed large savings in complexity can be achieved through optimized scheduling in a multiple concatenated scheme. Decoding in an iterative multiuser detector (IMUD) receiver proceeds according to a schedule of activations of the component decoders and interference canceller (IC). Conventional IMUD receivers follow a fixed (static) decoding schedule, which can be inefficient since it potentially adds more complexity and delay to the iterative decoding process than necessary. An IMUD receiver can therefore more efficiently use the physical resources if schedule optimization is used, that is, less turbo decoder (TD) iterations requires less power (clock speed can be reduced), and detection can be carried out by re-allocation of the physical resources to other users as they become available. In [5] and [6] the authors used EXIT charts to derive optimal decoding schedules for concatenated codes and an IMUD receiver respectively.

EXIT chart analysis based on an infinite block length results in a mismatch from trajectories simulated over a finite block length. This was observed in [4] where trajectory match was found to deteriorate over iterations. In [7] Li *et al* show an EXIT chart with confidence intervals and similarly, in [8] the authors propose a convergence analysis tool using a transfer characteristic band instead of a single transfer curve. Note that trajectory mismatch is not critical to convergence at high SNR, rather more so when operating close to the convergence threshold where the tunnel in the EXIT chart is narrow.

We propose dynamic decoding schedule optimization to fix the problem, that is, on each iteration of the receiver derive the optimal schedule to achieve a target bit error rate using a minimum number of turbo decoder iterations. By doing so, is is able to compensate for decoding trajectory mismatch. We compare the complexity of the scheduling algorithm with that of the MAP decoder used in the 3GPP TD. Furthermore, we investigate methods to reduce the complexity of the proposed algorithm.

Joint optimization of the power and decoding schedule is prohibitively complex so we break the optimization in two parts and first optimize power levels of each user then optimize the decoding schedule using the optimized power levels. In previous work [9] we optimized the power levels for a multiuser CDMA receiver with no consideration of the decoding schedule, while in [6] and [10] the decoding schedule was optimized with equal power levels. In this

Manuscript received May 29, 2007; revised September 23, 2007; accepted December 16, 2007. The associate editor coordinating the review of this paper and approving it for publication was H. Nguyen.

M. C. Reed, Z. Shi, and D. Shepherd are with National ICT Australia and affiliated with the Australian National University (e-mail: david.shepherd@anu.edu.au). National ICT Australia is funded through the Australian Governments Backing Australias Ability initiative and in part through the Australian Research Council.

F. Brännström is with the Department of Signals and Systems, Chalmers University of Technology.

F. Schreckenbach is with Munich University of Technology.

Digital Object Identifier 10.1109/T-WC.2008.070557

paper we show that there need not be any trade-off between complexity (number of iterations) and total power usage. Large gains in power efficiency and complexity can be achieved simultaneously. Furthermore, our optimized receiver has a lower convergence threshold and requires less iterations to achieve convergence than a conventional receiver. We show that our proposed optimization results in a more consistent quality of service (QoS).

The remainder of the paper is organized as follows. Section II gives an overview of the system model and Section III derives the EXIT functions for the receiver in the unequal power case. We optimize the power levels in Section IV and schedule in Section V. Simulation results are presented in Section VI and Section VII concludes the paper.

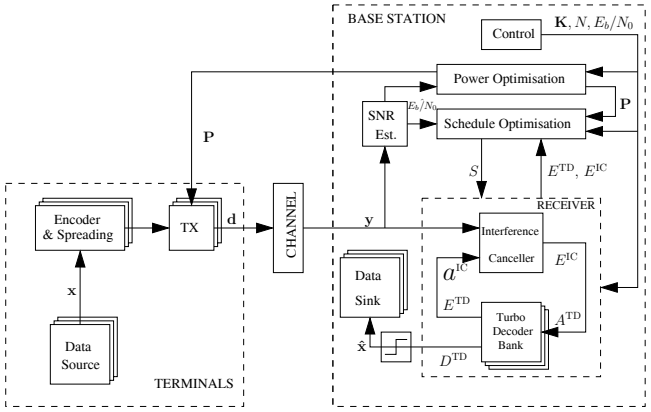


Fig. 1. IMUD receiver with control blocks (Power and Schedule Optimization), interference canceller and turbo decoders.

## II. System Description

We consider a turbo coded multiuser DS-CDMA system. However the work in this paper can be generalized for other iterative receivers. For the basic system model we refer the reader to [11]. There are $K$ transmitters generating independent data symbols $x_k \in \{-1, 1\}$ which are turbo encoded. The turbo code is 3GPP compliant, common for all users and consists of symmetric parallel concatenated 8-state convolutional codes with generator polynomial $(G_r, G) = (015, 013)$. The trellis is terminated in the encoders and the overall code rate is $R = 1/3$ (no puncturing) and information block lengths range from 40 up to 3856 bits [12]. We use 3856 bits for all simulations in this paper. The coded data $d_k \in \{-1, 1\}$ is interleaved and spread by direct-sequence spreaders $s_k \in \{-1/\sqrt{N}, +1/\sqrt{N}\}$ where $N$ is the processing gain (spreading factor). The outputs are mapped onto BPSK symbols, while the work in this paper can be analogously applied to higher-order modulation. The received signal is

$$y = \sum_{k=1}^{K} \sqrt{P_k} s_k d_k + n, \tag{1}$$

where $P_k$ is the power of user $k$ and $n$ is AWGN noise with variance $N_0/2$. The optimization techniques described in this paper are general and can be extended to the multipath fading channel. However, the derivation of the EXIT functions for the receiver blocks are non-trivial for the mobile channel. The problem is addressed in [13], however the application of the power and scheduling optimization to this scenario is intended for future work.

The IMUD receiver, shown in Fig. 1, consists of an IC and $K$ TDs and was first described for convolutional codes in [11]. See [4] for a good description of the turbo decoder. The interference canceller takes as inputs the channel values $y$ and *a priori* information $A^{\mathrm{IC}}$k (from each of the $K$ users $k = 1, 2, \ldots, K$) and outputs extrinsic information (on the coded bits for each user) $E_k^{\mathrm{IC}}$ which is de-interleaved and becomes the *a priori* input $A_k^{\mathrm{TD}}$ to the TD for user $k$. On the first iteration of the receiver the *a priori* input to the interference canceller is zero. Each of the $K$ TDs outputs extrinsic information (on the coded bits) $E_k^{\mathrm{TD}}$ and *a posteriori* output (on the information bits) $D_k^{\mathrm{TD}}$. $E_k^{\mathrm{TD}}$ is interleaved and converted to soft bits $A_k^{\mathrm{IC}} = \tanh(E_k^{\mathrm{TD}}/2)$. Hard decisions are made on $D_k^{\mathrm{TD}}$. Uppercase symbols are used to denote a log-likelihood ratio (LLR) and lowercase for soft bits.

A block diagram of the system is shown in Fig. 1. Also shown are the *control* blocks - Power Optimization, Schedule Optimization and the overall Control block which passes information such as number of users and spreading factor to each receiver block. Note that we have omitted the subscript $k$ for *a priori* and extrinsic data and have not shown the interleaver/deinterleaver between the IC and TD. The Power Optimization module passes the optimized power profile $\mathbf{P}$ to the transmitter and Schedule Optimization module. The optimal schedule information $S$ generated by the Schedule Optimization module is passed to the receiver.

The system functions as follows. For each input data block the power levels are optimized for the load and channel conditions. After transmission through the channel the noisy transmitted data is fed to the IC. After interference cancellation the dynamic schedule algorithm in Section V-D is run to estimate the optimal decoding schedule given the (estimated) point at which the decoding currently lies on the receiver EXIT chart. The scheduling algorithm may then be called upon after any subsequent IC activations, depending on the degree of trajectory mismatch. The major advantage of dynamic scheduling over static scheduling is that the method compensates for performance better/worse than expected (average) due to differences in channel conditions over decoding blocks, or differences in the decoding trajectory. Using dynamic scheduling we have a more reliable receiver for similar complexity.

## III. EXIT Chart Analysis

Consider a CDMA system with $L$ groups of different power levels. Define $\mathbf{K} = [K_1, K_2, ...K_L]$ and $\mathbf{P} = [P_1, P_2, ..., P_L]$, where $K_k$ and $P_k$ are the number of users in the group $k$ and their transmission power, respectively, for $k = 1, 2, \ldots, L$. The total number of users in the system is given by

$$K_T = \sum_{k=1}^{L} K_k. \tag{2}$$

We model the receiver blocks using variance and extrinsic information transfer functions. In an unequal power CDMA

system the users are grouped according to their power level. We assume all users within a power group are essentially identical and we therefore consider each group as a (virtual) single user. For convergence analysis, the traditional EXIT charts need to be adjusted to reflect the behavior of the system under the unequal power conditions [9], [14]. We assume hereafter the probability density functions of the input and output of the receiver blocks are Gaussian.

We utilize the $J$ function, which describes mutual information as a function of variance, from [4] where

$$I_\Lambda(\sigma_A) = J(\sigma_\Lambda = \sigma) \tag{3}$$

$$= 1 - \int_{-\infty}^{+\infty} \log_2\left(1+e^{-\xi}\right) \frac{1}{\sqrt{2\pi\sigma_A^2}} e^{\frac{-(\xi-\frac{\sigma_A^2}{2})^2}{2\sigma^2}} d\xi \tag{4}$$

and $\xi$ are the samples of $\Lambda$. Note that $\Lambda = \frac{\sigma_A^2}{2} d + n_\Lambda \sim \mathcal{N}(0, \sigma_\Lambda^2)$ and $\sigma_\Lambda^2 = 4/\sigma_\lambda^2$ where $\sigma_\lambda^2$ is the variance of the soft information $\lambda$. For the interference canceller, the *effective* EXIT function is [6]

$$I_{E,\text{eff}}^{\text{IC}} = f_{\text{mud}}\left(I_{A,\text{eff}}^{\text{IC}}, E_b/N_0\right) = J\left(\sqrt{\frac{4}{\left(1-T^{-1}\left(I_{A,\text{eff}}^{\text{IC}}\right)\right)\frac{K_{\text{eff}}-1}{N} + \frac{N_0}{2RP_{\text{ref}}}}}\right) \tag{5}$$

where $I_{A,\text{eff}}^{\text{IC}} = I_{E,\text{eff}}^{\text{TD}}$ is the effective prior mutual information for the IC (the extrinsic information from the TD), $K_{\text{eff}} = \frac{1}{P_{\text{ref}}}\sum_{k=1}^{L} K_k P_k$ is the effective number of users, $P_{\text{ref}}$ is some arbitrary reference power level (unless otherwise specified, $P_{\text{ref}} = P_1 = E_b$), $N$ is the processing gain, $R$ is the code rate and $T(.)$ is the transfer function from [15] which describes mutual information $I$ as a function of fidelity $M = \mathsf{E}\{(x-\hat{x})^2\}$,

$$I = T(M) \approx 0.74M + 0.26M^2. \tag{6}$$

$I_{E,\text{eff}}^{\text{IC}}$ is estimated online from the IC output using [14], [15]

$$\hat{I}_{E,\text{eff}}^{\text{IC}} = J\left(\sqrt{\frac{4}{\frac{1}{L}\sum_{k=1}^{L}\sigma_{k,E}^2}}\right) \tag{7}$$

where $\sigma_{k,E}^2 = \text{var}(e_k^{\text{IC}})$ is the variance of the soft output of the IC for user $k$. Note that the LLRs passed to the TD are generated as $E_k^{\text{IC}} = 2P_k e_k^{\text{IC}}/\sigma_{k,E}^2$. There are numerous methods in the literature for estimation of $\sigma_{k,E}^2$, we use the estimator proposed in [16].

We generate the EXIT chart for the TD, $I_E^{\text{TD}} = f_{\text{dec}}(I_A^{\text{TD}})$, using Monte Carlo simulation with $P_{\text{ref}} = 1$. The *effective* EXIT function for group $k$ with power $P_k$ is then

$$I_{E,k}^{\text{TD}} = f_{\text{dec}}\left(J\left(\sqrt{\frac{P_k}{P_{\text{ref}}}} J^{-1}\left(I_{A,\text{eff}}^{\text{TD}}\right)\right)\right), \tag{8}$$

where $I_{A,\text{eff}}^{\text{TD}} = I_{E,\text{eff}}^{\text{IC}}$ is the effective prior mutual information for the TDs. We estimate $I_{E,k}^{\text{TD}}$ and $I_{D,k}^{\text{TD}}$ online using [17]

$$\hat{I}_{\Lambda,k}^{\text{TD}} = 1 - 2\mathsf{E}\left\{\frac{\log_2\left(1+e^{-\Lambda_k^{\text{TD}}}\right)}{1+e^{-\Lambda_k^{\text{TD}}}}\right\}, \tag{9}$$

where $\Lambda$ is $E$ or $D$. The *effective* mutual information of the extrinsic output of the $K$ TDs is calculated as [6]

$$I_{E,\text{eff}}^{\text{TD}} = 0.74\left[1-\sum_{k=1}^{L}\alpha_k^*\left(2.42-\sqrt{2.03+\frac{I_{E,k}^{\text{TD}}}{0.26}}\right)\right] + 0.26\left[1-\sum_{k=1}^{L}\alpha_k^*\left(2.42-\sqrt{2.03+\frac{I_{E,k}^{\text{TD}}}{0.26}}\right)\right]^2, \tag{10}$$

where the decoder outputs are weighted using

$$\alpha_k^* = \frac{K_k P_k}{K_{\text{eff}} P_{\text{ref}}}. \tag{11}$$

Now using (8) and (10) we express the *effective* TD EXIT chart as

$$I_{E,\text{eff}}^{\text{TD}} = f_{\text{dec}}^*\left(I_{A,\text{eff}}^{\text{TD}}\right). \tag{12}$$

Note that we derive the EXIT chart of the TD for $i^d \in (1,2,...,i_{\max}^d)$ iterations where $i_{\max}^d$ is the maximum number of TD iterations. We also derive the EXIT function of the TD considering only the systematic bits, denoted by $E(s)$, which we use for bit-error-rate (BER) estimation. We have observed a small difference between $I_{E(s)}^{\text{TD}}$ and $I_E^{\text{TD}}$.

In this paper we focus on unequal power CDMA. However, the techniques described can be extended to systems utilizing adaptive modulation and coding. EXIT charts have been used for irregular codes in [18] for example, where a system was optimized by the selection of codes from an ensemble of different rate codes. In [19] EXIT charts were used to optimize bit-interleaved coded irregular modulation. The key concept is the ability to construct *effective* EXIT functions, that is a single EXIT function to represent the transfer function of a group users with different power, code rate, or modulation.

## IV. Power Optimization

For a mobile system operator power optimization has the following benefits;

- longer battery life in user terminal
- less interference allowing larger cell sizes
- more users per cell.

We therefore want to minimize the sum power of all users, which we address in this section. In multi-user CDMA system the convergence threshold, i.e. the SNR at which all users can decode successfully, depends on the power profile of the users. We consider a 3GPP compliant system where users can be grouped according to their power levels. Given the number of users $\mathbf{K} = [K_1, K_2, ..., K_L]$ in $L$ groups with spreading factor $N$, we propose a method to minimize the total power under the constraint that the system must converge. This approach essentially minimizes the convergence threshold given a total power by optimizing the distribution of power among the groups.

Once the IMUD receiver has been modelled using *effective* EXIT charts we are able to optimize the power levels of each group of users. Define the vector $\mathbf{z} = [0, \delta, ..., 1-\delta, 1]$ where

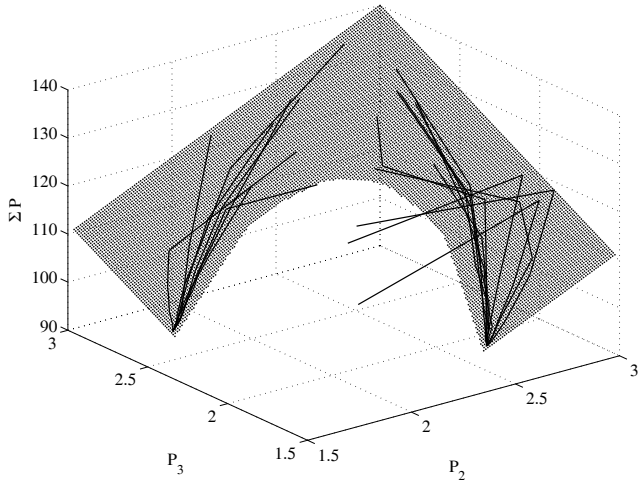


Fig. 2. Power optimization algorithm trajectory for random starting points.

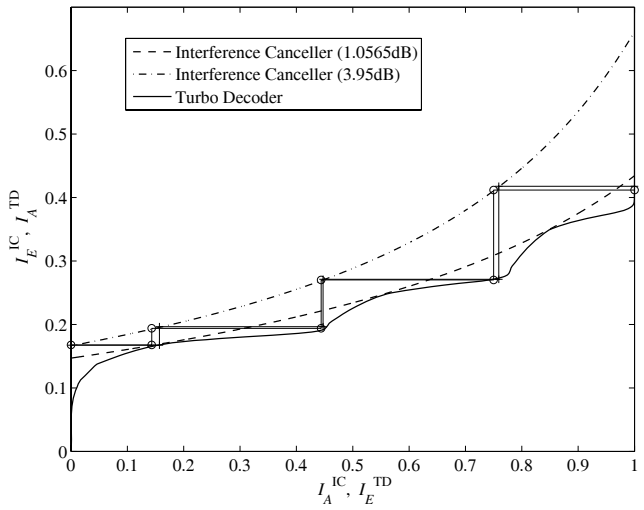


Fig. 3. EXIT chart for power optimized system $\mathbf{K} = [20, 20, 20]$, $N = 30$ and $\mathbf{P} = [1, 1.5381, 2.3917]$ at $P_{\text{ref}}/N_0 = 1.06$ and 3.95dB, and snapshot trajectories at $P_{\text{ref}}/N_0 = 3.95$dB.

$\delta \ll 1$ is arbitrarily selected for resolution and the entries of $\mathbf{z}$ correspond to the MI $I_{A,\text{eff}}^{\text{IC}} = I_{E,\text{eff}}^{\text{TD}}$, such that

$$I_{E,\text{eff}}^{\text{IC}} = f_{\text{mud}}(z) \tag{13}$$

$$I_{A,\text{eff}}^{\text{TD}} = f_{\text{dec}}^{*-1}(z) \tag{14}$$

where $z \in \mathbf{z}$. We can use (13) and (14) to observe the (predicted) convergence properties of the transfer chart. That is, we can use $\text{sgn}(f_{\text{mud}}(z) - f_{\text{dec}}^{*-1}(z))$ to determine whether the transfer curves intersect and $||f_{\text{mud}}(z) - f_{\text{dec}}^{*-1}(z)||$ to calculate the width of the tunnel. The optimization determines the power allocation which minimizes total transmit power given that a tunnel must be open in the EXIT chart such that iterative decoding can proceed until all multi-access interference (MAI) is removed.

We define the cost function as

$$F(\mathbf{P}) = \sum_{k}^{L} K_k P_k \tag{15}$$

where the goal of the optimization is to minimize $F(\mathbf{P})$. That is

$$\min_{\mathbf{P}} F(\mathbf{P})$$

$$\text{subject to} \begin{cases} b_l < P_k < b_u, & \forall k \\ c(\mathbf{P}) \leq 0 \end{cases}$$

where $b_l$ and $b_u$ are the lower and upper bounds (respectively) imposed on the optimization variable $\mathbf{P}$ by the receiver and $c(\mathbf{P})$ is the nonlinear constraint function

$$c(\mathbf{P}) = f_{\text{mud}}(z) - f_{\text{dec}}^{*-1}(z) + \Delta \tag{16}$$

where $\Delta$ is an arbitrary scalar which represents the open tunnel between the two transfer curves. We show in Fig. 2 a map of the optimization space obtained through a brute-force search over all possible power profiles for a 3 power-group ($\mathbf{K} = [20, 20, 20]$ and $N = 30$) system where $P_1 = P_{\text{ref}} = 1$. The inclined plane represents the set of points where the power profile allows successful decoding (open tunnel in the EXIT chart). We also show the trajectory of the algorithm for the power optimization (using random start points) using an optimization algorithm based on the interior-reflective Newton method [20], [21] and we see that the optimization converges on 2 solutions. The solution is therefore not guaranteed to be optimal. However, we have provided the framework for the optimization and leave the selection of a superior algorithm for future work.

Fig. 3 shows the EXIT chart for a power-optimized unequal power CDMA system, $\mathbf{K} = [20, 20, 20]$ and $N = 30$, we see that the EXIT curves match quite closely. The average SNR $\bar{E}_b/N_0$ is 2.95dB ($P_{\text{ref}}/N_0 = 1.06$dB) at the solution $\mathbf{P}' = [1, 1.5381, 2.3917]$, shown by the dashed line (IC) and solid line (TD).

## V. Scheduling

The activation order, or scheduling, of receiver components is essential in the design of an iterative receiver with multiple concatenated components. We adapt a trellis-based Viterbi search optimization algorithm for unequal power CDMA to optimize the decoding schedule such that the decoding complexity and delay (total number of TD iterations) are minimized while BER performance is maintained. The search algorithm is generalized for use in all concatenated receivers as it is able to account for an arbitrary starting point ($I_{A,\text{eff}}^{\text{IC}} \neq 0$) and the cost function is two-dimensional. A decoding trellis is shown in Fig. 4 for a CDMA system with two groups where each group can run either 1 or 6 iterations of the TD. The subscripts in $\text{TD}_{k,i}$ denote power-level group ($k$) and number of turbo decoding iterations ($i$). Each state in the trellis corresponds to activating the component represented by that state.

Note that the trellis can be fully connected, however the trellis in Fig. 4 is trimmed to reduce the complexity of the scheduling algorithm. We have manually removed redundant edges, such as from state 1 to state 1 (IC - IC), which achieve no gain in MI and would be removed by the algorithm itself. We derive the optimal schedule on each iteration of the receiver to compensate for differences between the predicted and actual EXIT chart trajectories.

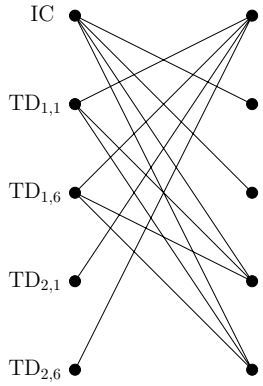


Fig. 4. Decoding trellis for two groups, where each state corresponds to activating a receiver component (IC or $\text{TD}_{k,i}$ where $k$ is power-level group and $i$ is the number of iterations).

### A. Static Scheduling

If the optimal schedule is derived off-line over a range of $P_{\text{ref}}/N_0$ values, the decoding schedule can be determined in two ways;

- use the optimal schedule at the convergence threshold for all SNR
- estimate the SNR online and use a look-up table to select the optimal schedule.

The first option assumes only that the system configuration ($K$, $N$ and $P$) is known. The latter has the additional requirement that SNR be estimated. See Table I for an example of a schedule look-up table. Noting in (5) that the SNR is needed to derive the IC EXIT chart, we propose a novel method of estimating the SNR in the AWGN CDMA channel. We first estimate the MI at the output of the IC $I_{E,\text{eff}}^{\text{IC}}$, using (7), after the first activation of the IC. Note that the first activation of the IC involves no cancellation and $E^{\text{IC}}$ is simply the match-filtered channel output. The SNR can then be estimated as

$$\frac{P_{\text{ref}}}{N_0} \approx \left( 2R \left( \frac{4}{J^{-1}\left(I_{E,\text{eff}}^{\text{IC}}\right)^2} - \frac{K_{\text{eff}}-1}{N} \right) \right)^{-1}, \qquad (17)$$

which we obtained using (5). We have found the mismatch in trajectories to be negligible following the first activation of the IC, so estimating the SNR and deriving the IC EXIT function in this method is sufficiently accurate.

### B. Dynamic Scheduling

Alternatively the schedule can be derived dynamically to compensate for variations in the decoding trajectory. EXIT charts assume the interleaver depth is large so when small block lengths are used there is mismatch between the expected and simulated trajectories [4]. The schedule can be dynamically derived following every $x^{\text{th}}$ IC activation. The frequency of schedule refining depends upon the degree of variation in the decoding trajectory. Some decision criteria can be used to determine whether the mismatch is sufficient to require refining of the schedule, for example deviation from the expected $I_D$, where

$$I_D = J\left( \sqrt{J^{-1}\left(I_{E,\text{eff}}^{\text{IC}}\right)^2 + J^{-1}\left(I_{E,\text{eff}}^{\text{TD}}\right)^2} \right). \qquad (18)$$

### C. Notation

Let $m$ denote trellis transition. Each group is permitted $i^d \in \{1, 2, ..., i_{\max}^d\}$ iterations. Paths entering state $n$ are defined as $\mathbf{p}_r = (p_1, p_2, ..., p_m)$ where $r \in [0, \infty)$ is the path number, $p_j \in \{1, 2, ..., i_{\max}^d L + 1\}$ for $1 \le j \le m-1$ and $p_m = n$. The metric for the corresponding path is represented as $\mathbf{v} = (v_1, v_2, ..., v_{2L+4})$, which we define as

$$\mathbf{v} = (\hat{P}_{b,1}, \ldots, \hat{P}_{b,L}, C^{\text{IC}}, C^{\text{TD}}, I_{E,\text{eff}}^{\text{IC}}, I_{E,\text{eff}}^{\text{TD}}, I_{E,1}^{\text{TD}}, \ldots, I_{E,L}^{\text{TD}}) \qquad (19)$$

where complexity $C^{\text{IC}}$ is the number of receiver iterations (IC activations) and $C^{\text{TD}}$ is the total number of TD iterations. Complexity is updated as

$$C_m^{\text{IC}} = C_{m-1}^{\text{IC}} + \begin{cases} 1 & \text{for an IC activation} \\ 0 & \text{otherwise,} \end{cases} \qquad (20)$$

$$C_m^{\text{TD}} = C_{m-1}^{\text{TD}} + \begin{cases} i^d & \text{for a TD activation} \\ 0 & \text{otherwise,} \end{cases} \qquad (21)$$

where $i^d$ is the number of TD iterations. The receiver is permitted $i^r \in \{1, 2, ...i_{\max}^r\}$ iterations.

Note that the complexity metric is two-dimensional in contrast to one-dimension in [5]. This is due to our constraint on $i^r$.

Let $I_{D,k}$ denote the mutual information of the *a posteriori* output from TD group $k$. It can be calculated as

$$I_{D,k} = J\left( \sqrt{J^{-1}\left(I_{A(s),k}^{\text{TD}}\right)^2 + J^{-1}\left(I_{E(s),k}^{\text{TD}}\right)^2} \right) \qquad (22)$$

where $A(s)$ and $E(s)$ denote the *a priori* and extrinsic mutual information of the systematic bits, respectively. The expression in (22) can be used to estimate the BER of group $k$ as [4]

$$\hat{P}_{b,k} = Q(J^{-1}(I_{D,k})/2), \qquad (23)$$

which are the $L$ first elements in (19). Since $\sigma_D^2 = \sigma_A^2 + \sigma_E^2$, the point on the EXIT chart at which a paths trajectory finishes is described by $I_D$ in (18), which we can use as a single metric to gauge path performance in complexity saving techniques which are described in Section VI. The convergence point $I_D^*$ is the point where the IC and TD EXIT functions intersect and the convergence BER $P^* = Q\left(J^{-1}(I_D^*)/2\right)$ the corresponding BER.

The sets of surviving paths and metrics are denoted by $\mathcal{P}_m$ and $\mathcal{V}_m$ respectively; and $\mathcal{P}_{m,n} \subseteq \mathcal{P}_m$ and $\mathcal{V}_{m,n} \subseteq \mathcal{V}_m$ are the sets of paths and metrics ending at state $n$ after $m$ trellis transitions. The current (at transition $m$) optimal path $\mathbf{p}^*$ has metric $\mathbf{v}^*$. The number of paths in $\mathcal{P}_m$ is denoted by $R$.

The start point of the algorithm is determined using the metric initialization function $f_{\text{init}}(E_k^{\text{IC}}, E_k^{\text{TD}}, D_k^{\text{TD}})$, where $I_{E,\text{eff}}^{\text{IC}}$ is updated using (7), $I_{E,k}^{\text{TD}}$ and $I_{D,k}^{\text{TD}}$ using (9) and $I_{E,\text{eff}}^{\text{TD}}$ using (10). This is done on-line after activation of the IC using the current $E_k^{\text{IC}}$, $E_k^{\text{TD}}$ and $D_k^{\text{TD}}$. Note that performance of

TABLE I
SCHEDULE LOOK-UP TABLE FOR $\mathbf{K} = [20, 20, 20]$, $N = 30$, $\mathbf{P} = [1, 1.5381, 2.3917]$, WHERE EACH SCHEDULE REPRESENTS A PATH THROUGH THE TRELLIS OF FIG. 4.

| $E_b/N_0$ (dB) | Schedule ($S$) |
|---|---|
| 3.95 | $IC, TD_{1,1}, TD_{2,2}, TD_{3,6}, IC, TD_{1,2}, TD_{2,3}, TD_{3,6}, IC, TD_{1,2}, TD_{2,6}, TD_{3,3}, IC, TD_{1,6}, TD_{2,2}$ |
| 4 | $IC, TD_{2,1}, TD_{3,4}, IC, TD_{1,1}, TD_{2,2}, TD_{3,6}, IC, TD_{1,2}, TD_{2,6}, TD_{3,3}, IC, TD_{1,6}, TD_{2,2}$ |
| 5 | $IC, TD_{2,1}, TD_{3,2}, IC, TD_{3,5}, IC, TD_{2,5}, IC, TD_{1,5}, TD_{2,2}, TD_{3,1}$ |
| 6 | $IC, TD_{3,2}, IC, TD_{2,1}, TD_{3,5}, IC, TD_{2,5}, IC, TD_{1,3}$ |

the algorithm is highly dependent upon the reliability of the output of $f_{\text{init}}$ which defines the point on the EXIT chart from which the decoding path begins. If $f_{\text{init}}$ overestimates mutual information the schedule will not allocate sufficient iterations and vice versa.

The metric update function $f_n(I_{E,\text{eff}}^{\text{IC}}, I_{E,k}^{\text{TD}}, i^d)$, for each state $n$ [5], is used to update the $2L+4$ elements in $\mathbf{v}$ for all paths entering state $n$ using (5), (8), (10), (23) and (21). This function uses look-up tables (of the receiver block EXIT functions) to estimate the path's trajectory on the EXIT chart corresponding to the transition through the trellis.

We define domination as in [5], where metric $\mathbf{v}$ dominates $\mathbf{v}'$ if and only if the extrinsic mutual information $v_q$ are higher than $v_q'$ for $q = L+3, L+4, \ldots, 2L+4$, respectively, and the complexities $v_q$ are less than or equal to $v_q'$ for $q = L+1, L+2$. Define target BER $P_{\text{target}}$ as the desired BER of each group of users.

### D. Algorithm

The algorithm is divided into 2 parts - an off-line initialization and the on-line Viterbi search. The initialization procedures are as follows

1) Derive the EXIT chart for the load/power/SNR configuration of interest using the results from Section III (note that $I_E = f_{\text{dec}}(I_A)$ must be generated using Monte Carlo simulation)
2) Determine the convergence point $I_D^*$, the intersection of the TD EXIT (for $i_{\max}^d$ iterations) curve with the interference canceller curve
3) Calculate the convergence BER $P^* = Q(J^{-1}(I_D^*)/2)$

The Viterbi search algorithm is as follows

1) Let $m = 1$. Initialize path set to contain only one path $\mathcal{P}_= \{(1)\}$ and corresponding metric set $\mathcal{V}_m = \{f_{\text{init}}\}$. Initialize $\mathbf{p}^* = 1$ and $v_{L+1}^* = v_{L+2}^* = \infty$.
2) $m = m + 1$, calculate the number of paths $R$ in $\mathcal{P}_m$. For each state $n'$ extend each path $\mathbf{p}_r'$ ending in state $n'$ along the trellis defined transition $n' \to n$, producing the new path $\mathbf{p}_{R+1}$ in $\mathcal{P}_{m,n}$, update the metric in $\mathcal{V}_{m,n}$ using $\mathbf{v} = f_n(\mathbf{v}')$ and increment $R$.
3) Define a set of metrics $\mathcal{V}^*$ for paths that have reached the target BER ($v_q \le P_{\text{target}}$, $\forall\ q = 1, 2, \ldots, L$), the convergence point $I_D^*$ or $i_{\max}^r$ receiver iterations. If there are multiple paths in $\mathcal{V}^*$ replace the candidate path $\mathbf{p}^*$ with the path of the lowest complexity $v_{L+2}$.
4) For each state, eliminate dominated metrics and their corresponding paths. If $P^* < P_{\text{target}}$ eliminate paths in $\mathcal{V}^*$ with any $(\hat{P}_{b,1}, \hat{P}_{b,2}, ..., \hat{P}_{b,L}) > P_{\text{target}}$.
5) If no paths remain in $\mathcal{V}_m$ the candidate path $\mathbf{p}^*$ is the optimal path. Otherwise go to step 2.

### E. Complexity

One factor to consider is the complexity of the scheduling algorithm in comparison to the complexity savings realized. With a large number of groups $N_K$ and a large number of TD iterations ($i^d$) the number of states and surviving paths in the trellis can grow large. Though it is possible that the number of surviving paths in the algorithm grows exponentially, this has not been observed in practice.

The number of states in the trellis is $N_s = \nu_i^d N_K + 1$, where $\nu_i^d$ is the number of allowed TD iterations $i^d$ (e.g. $\nu_i^d = 6$ when $i_d \in \{1,2,...,5,6\}$), and the number of trellis transitions $N_T$ is $i_{\max}^r(N_K + 1)$. The complexity of the scheduling algorithm is approximately

$$O\left(N_s^{N_T}\right) \tag{24}$$

in the worst-case scenario, that is assuming no paths are removed in the domination step. With typical parameters $i_{\max}^r = 4$, $i^d \in \{1, 2, ..., 6\}$ and $N_K = 3$ the scheduling algorithm has complexity in the order of $10^{20}$. While the domination step generally ensures the complexity does not grow exponentially, the complexity of the scheduling algorithm is an issue, and measures such as

- trimming the trellis (remove redundant edges)
- reducing the number of survivor paths (e.g. keep only paths with $I_D \ge x \cdot I_D^{\max}$ where $x \in \{0, 1\}$) as in the $T$-BCJR algorithm [22]
- limiting the number of survivor paths (e.g. keep only best $x$ paths ranked in order of $I_D$ (18)) as in the $M$-BCJR algorithm [22]
- truncating the number of allowed TD iterations $i^d$ to some subset of $i^d$
- running scheduling algorithm every $x^{\text{th}}$ receiver iteration where $x > 1$

can be explored to resolve the problem. Preliminary work shows these methods offer potential for good complexity/performance trade-offs. For all work in this paper we utilize a trimmed trellis as shown in Fig. 4, where redundant edges have been removed and the system is forced to activate TDs in order (i.e. group 1,2,...,$N_K$). We use this approach alone, as it has no detrimental effect on the algorithm as the groups are independent. The other methods described may result in a sub-optimal schedule being selected. The $T$-BCJR algorithm is known to give near-optimum performance but fails to reduce worst-case complexity, while the $M$-BCJR algorithm reduces worst-case complexity but suffers from performance degradation [23]. Using a trimmed trellis the complexity is approximately

$$O\left(N_s \cdot \beta^{N_T - 1}\right) \tag{25}$$

where

$$\beta = \frac{N_s}{\text{mean number of edges per state}}. \tag{26}$$

With some careful trimming in the $K_T$ system we can reduce the number of edges from $(K_T \cdot \nu_i^d)^2 = 361$ to 39 and reduce the complexity of the scheduling algorithm to the order of $10^5$. Note that this is still worst-case (no removal of paths through domination) so in practice the complexity of the scheduling algorithm is lower than this. For a fully connected trellis (i.e. worst-case) the BCJR algorithm has complexity in the order of

$$O\left(\eta^2 \kappa\right) \tag{27}$$

where $\eta$ is the number of states in the 3GPP convolutional code trellis and $\kappa$ is the number of trellis transitions. In our 3GPP compliant system there are two edges per state in the trellis so the BCJR algorithm has complexity $O\left(2\eta\kappa\right)$. Since $\eta = 8$ and $\kappa = 3856$ the MAP decoder in the CDMA receiver in Fig. 1 therefore has complexity in the order of $10^4$. The proposed scheduling algorithm has (in the worst case) complexity one order of magnitude higher than that of one BCJR algorithm activation in the decoder. Remembering that one TD iteration requires two activations of the BCJR algorithm, in the worst-case the savings outweigh the cost if the scheduling algorithm can save at least five TD iterations.

## VI. Simulation Results

Unless specified otherwise, all BER values are the system average, calculated as

$$\hat{P}_b = \frac{1}{K_T} \sum_{k=1}^{L} K_k \hat{P}_{b,k}, \tag{28}$$

where $\hat{P}_{b,k}$ is the estimated BER for group $k$. We simulated two systems with $K_T = 60$ users and spreading factor $N = 30$, first with equal power (i.e. un-optimized) then with the optimized power levels for $N_K = 3$ power groups from Section IV. In consideration of the performance of a practical receiver, we define the 4-iteration threshold as the SNR required to allow convergence within 4 receiver iterations. For a system to operate at the convergence threshold a large number of iterations is required and the system has to perform to expectations if the EXIT trajectory is to pass through the tunnel between the EXIT curves. We consider the 4-iteration threshold to be more meaningful in terms of comparing performance of various system configurations. Note that the optimization algorithms and thresholds are defined such that all user groups achieve the target BER.

Recall that in general $P_{\text{ref}} = P_1$, we calculate the average SNR as

$$\bar{E_b}/N_0 = \frac{1}{N_K} \sum_{k=1}^{L} K_k \left( \frac{P_{\text{ref}}}{N_0} + \frac{P_k}{P_{\text{ref}}} \right), \tag{29}$$

where $P_{\text{ref}}/N_0$ and $P_k/P_{\text{ref}}$ are in dB, which we use to compare systems with different power profiles $\mathbf{P}$.

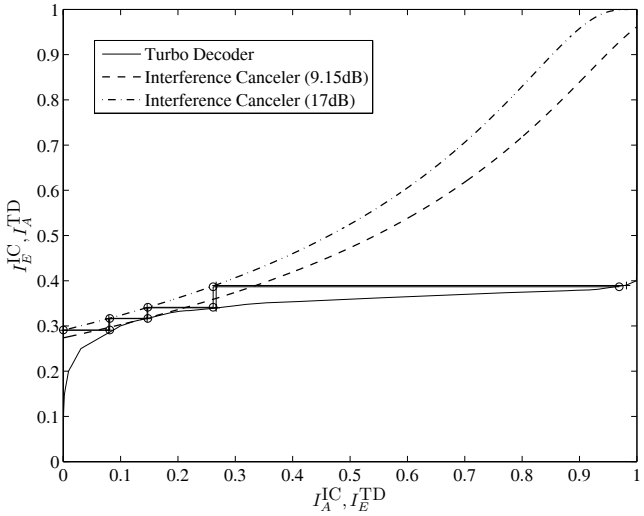


Fig. 5. EXIT chart for equal power $\mathbf{K} = 60$, $N = 30$ system at $P_{\text{ref}}/N_0 = 9.15$ and 17dB (the 4-iteration threshold).

### A. Equal Power System

We consider a heavily loaded ($\mathbf{K} = [60], \mathbf{P} = [1], N = 30$) equal power system. EXIT chart analysis in Fig. 5 shows the convergence threshold (dashed line) occurs at an SNR of $P_{\text{ref}}/N_0 = \bar{E_b}/N_0 = 9.17$dB and the 4-iteration threshold (dot-dashed line) at 17dB. We observe that the EXIT characteristics of the TD cause the bottleneck in this equal power system. The receiver would exhibit a sharp drop in BER over iterations once decoding has progressed through the narrow tunnel.

### B. Optimized System

A turbo coded unequal power CDMA system was simulated with $\mathbf{K} = [20, 20, 20]$ users, spreading factor $N = 30$ and optimized power $\mathbf{P} = [1, 1.5381, 2.3917]$. According to EXIT chart analysis in Fig. 3 the convergence threshold of this system is at $P_{\text{ref}}/N_0 = 1.06$dB (average SNR $\bar{E_b}/N_0 = 2.95$dB) and the 4-iteration threshold is at $P_{\text{ref}}/N_0 = 3.95$dB. We simulated the system over a range of SNR in the region of the 4-iteration threshold. Note that if $P$ was optimized with a constraint on $\Delta$ in (16) to be sufficiently large to allow convergence within 4 receiver iterations we obtain the same relative result $\mathbf{P}'$ but higher $P_1 = P_{\text{ref}}$, such that $P_{\text{ref}}/N_0 = 3.95$dB as above. Using (29) the average SNR at the 4-iteration threshold is $\bar{E_b}/N_0 = 5.84$dB, which corresponds to a 8.46dB gain over the equal power system.

As suggested in [5], the optimal schedule at the convergence threshold was chosen for all $P_{\text{ref}}/N_0$ in the simulation. This schedule will be referred to as the static (optimal) schedule. We set the full decoding schedule as all groups running 6 TD iterations and 4 receiver iterations.

The corresponding EXIT chart snapshot trajectories are shown in Fig. 3 at $P_{\text{ref}}/N_0 = 3.95$dB. Both snapshot trajectories match quite closely with EXIT chart analysis. Since the EXIT functions described in Section III assume a large-scale system (PDF of MAI is approximately Gaussian) and the block length is finite, we expect some performance dif-

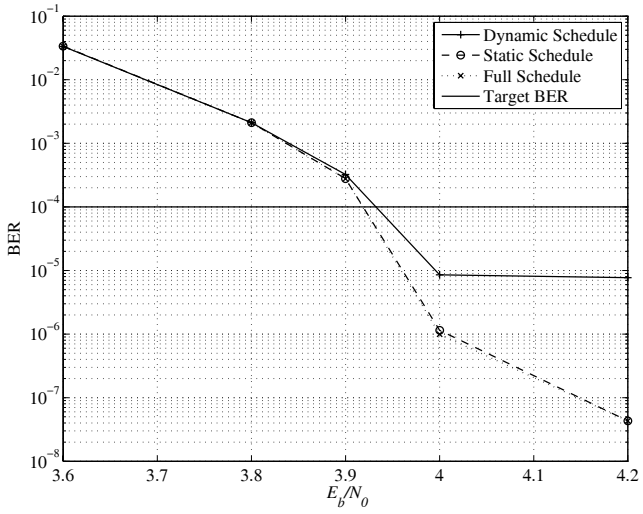


Fig. 6. BER performance of unequal power CDMA system $\mathbf{K} = [20, 20, 20]$, $\mathbf{P} = [1, 1.5381, 2.3917]$ and $N = 30$ for IMUD receiver following the dynamic, static and full decoding schedules.

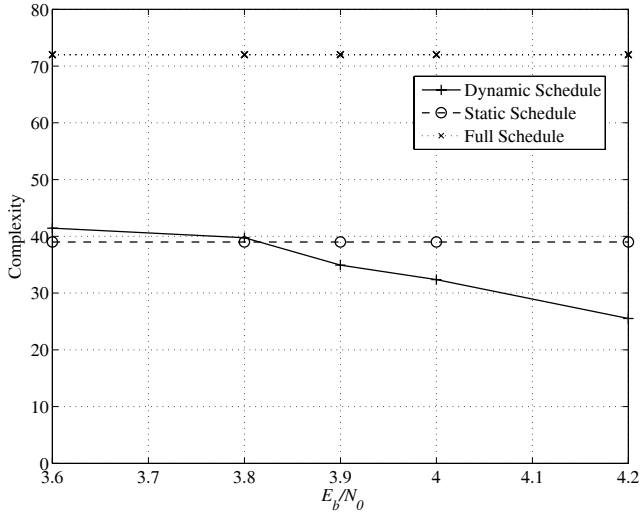


Fig. 7. Complexity of unequal power CDMA system $\mathbf{K} = [20, 20, 20]$, $\mathbf{P} = [1, 1.5381, 2.3917]$ and $N = 30$ for IMUD receiver following the dynamic, static and full decoding schedules.

ferences between this system and the asymptotic performance predicted.

BER performance is plotted versus SNR in Fig. 6, where we see that BER performance of the dynamic schedule is very similar to that for the full decoding schedule up to the convergence threshold. The target BER $P_{\text{target}}$ is $10^{-4}$ so dynamic scheduling exhibits an error floor below $P_{\text{target}}$ for SNR above the convergence threshold. Note that the error floor is not exactly equal to $P_{\text{target}}$, which is due to the shape of the TD EXIT function. As seen in Fig. 3, the TD EXIT function approaches high values of $I_E^{\text{TD}}$ close to horizontally, so there is a very sharp drop from high to very low BER.

We observe that static scheduling also achieves very similar BER performance despite the static schedule being optimized only for the convergence threshold. This can be easily understood using the EXIT chart Fig. 3 and the EXIT function for the TD at low $I_A^{\text{TD}}$. At low SNR the IC and TD EXIT functions intersect at low $I_{A,\text{eff}}^{\text{TD}}$ and in this region the TD EXIT function is very similar for all $i^d$. Therefore the system will come close to the convergence point following almost any schedule. If we consider an EXIT chart BER contour plot [4], at low values of MI the BER contours are widely spaced, i.e. large gain in MI achieve only a small improvement in BER, thus very little difference in BER will be seen between schedules in these cases. For high SNR the tunnel between the EXIT functions opens further so decoding following any schedule optimized for low SNR (i.e. a narrow tunnel) will easily step through the tunnel. This is inefficient as similar BER performance can be achieved with less TD/receiver iterations and explains why dynamic scheduling significantly reduces complexity at high SNR. This can be seen in Fig. 7, where we show the complexity required to achieve the corresponding BERs from Fig. 6. The static schedule achieves approximately a 45% reduction in complexity for similar BER performance as the full schedule. Using dynamic scheduling further savings in complexity are achieved, with savings increasing with SNR up to 64% compared to the full schedule at 4.2dB. Note that below the convergence threshold dynamic scheduling uses more TD iterations than the static schedule. This is only due to the fact that the static schedule is derived at the convergence threshold. An ARQ scheme could be investigated as possible extension of this work, as complexity could be further reduced for packets where $P^* > P_{\text{target}}$ by discarding the packet. Note the presence of an error floor for dynamic scheduling for $E_b/N_0 \geq 4$dB (i.e. above the convergence threshold), which is due to the target BER defined in the scheduling algorithm. The error floor is approximately equal to $P_{\text{target}}$.

We note in Fig. 6 that the BER performance for dynamic and static scheduling is approximately equal. However, while the mean BER is equal the variance is less for dynamic scheduling. Using dynamic scheduling less *packets* (data blocks) fail to achieve the target BER. Specifically, at 4dB for example, 96.5% of packets achieved the target while static scheduling achieved the target in only 86.9% of packets.

### C. Power vs Complexity

In Fig. 8 we show the complexity required to achieve a target BER $P_{\text{target}}$ of $10^{-4}$ in a CDMA system with $K_T = 60$ users and processing gain $N = 30$. This graph allows the user to select a complexity vs power trade-off. As average SNR is decreased more iterations are required to achieve convergence and vice versa. We show four cases in Fig. 8,

- No Optimization: equal power and no scheduling; $i^d = 6$ and iterate receiver until no further decrease in BER
- Power Optimized: $\mathbf{P} = \mathbf{P}'$ and no scheduling; $i^d = 6$ and iterate receiver until no further decrease in BER
- Schedule Optimized: equal power and dynamic scheduling
- Power + Schedule Optimized: $\mathbf{P} = \mathbf{P}'$ and dynamic scheduling.

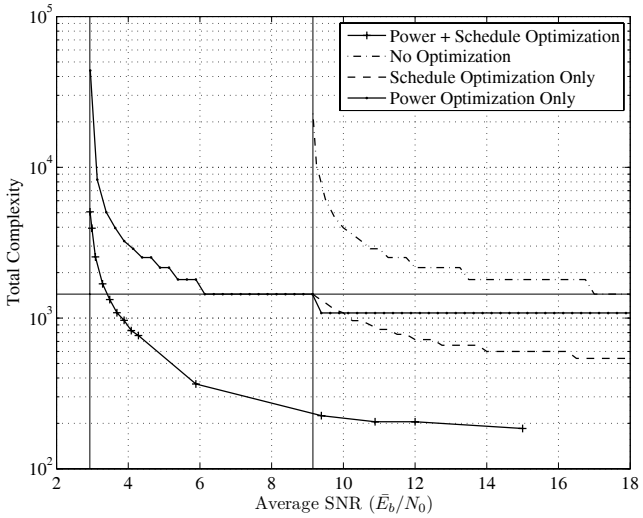


Fig. 8. Average SNR vs Total Complexity for power, schedule (and combined power/schedule) optimization, using a target BER of $10^{-4}$.

Total complexity is shown on the $y$-axis where total complexity is calculated as

$$C_{\text{total}} = \begin{cases} \sum_{k=1}^{N_K} K_k \cdot i^d \cdot i^r & \text{without scheduling} \\ \sum_{k=1}^{N_K} K_k \cdot i^d \cdot i^r + \phi & \text{with scheduling,} \end{cases} \quad (30)$$

where $\phi = 5$ is obtained using the results in Section V-E. In the no optimization case ($\mathbf{K} = [60]$, $\mathbf{P} = [1]$), shown by the dot-dashed line, we see the convergence threshold occurs at an average SNR of $\bar{E}_b/N_0 = 9.15$dB and the complexity $C_{\text{total}}$ is high. If the users are split into 3 equal size groups and the power levels are optimized as above, $\mathbf{K} = [20, 20, 20]$ and $\mathbf{P} = [1, 1.5381, 2.3917]$, we obtain the dotted line in Fig. 8. The convergence threshold is reduced such that $P_{\text{target}}$ is achieved at an average SNR of $\bar{E}_b/N_0 = 2.95$dB, however, the complexity remains high.

If alternatively the schedule is optimized the complexity can be reduced by more than $50\%$ as shown by the dashed line. As each user has equal power the convergence threshold remains unchanged from the no optimization case.

The solid line shows the performance of the power and schedule optimized receiver, which we see has significant complexity and power gains over the conventional receiver. Note there no trade-off made between complexity and power. The receiver is able to operate more efficiently in the lower left region of Fig. 8.

The convergence threshold is the vertical asymptote to the left of each curve, where complexity grows towards infinity. The average SNR of each asymptote in Fig. 8 corresponds to the SNR at which the two component EXIT functions intersect in the EXIT charts.The upper left end of the no optimization curve (dot-dash) in Fig. 8 corresponds to the lower TD EXIT function in Fig. 5. While successful decoding is possible, the tunnel is narrow and a large number of iterations are required to achieve convergence. Similarly, in the power optimized system (dots), the upper left end of the curve corresponds to the TD and lower IC EXIT functions in Fig. 3.

The horizontal line in Fig. 8 corresponds to the 4-iteration threshold where the normalized complexity is equal to $C_{\text{total}} = 1440$ TD iterations, where $i^d = 6$ and $i^r = 4$ which are assumed to be reasonable values in consideration of a practical system. According to the upper TD EXIT function in Fig. 5 the 4-iteration threshold occurs at 17dB in the equal power system. This corresponds to the point the no optimization curve intersects with the 4-iteration threshold at $\bar{E}_b/N_0 = 17$dB. The power optimized system achieves the target BER $P_{\text{target}}$ in 4 receiver iterations at an average SNR of $\bar{E}_b/N_0 = 5.84$dB which is seen in Fig. 8 where the power optimized curve crosses the horizontal 4-iteration threshold line. This point is represented by the upper TD EXIT function in Fig. 3. For the schedule optimized curves the complexity represents the total average receiver complexity, it is not possible to infer the number of receiver iterations as $i^r$ and and $i^d$ are dynamically allocated by the algorithm.

## VII. Conclusion

We have optimized a turbo MUD receiver for unequal power turbo-coded CDMA system through EXIT chart analysis. The results in [14] were used to derive *effective* EXIT functions for FEC decoders and an interference canceller which enabled analysis of the system as in the equal power case. We utilized a nonlinear constrained optimization as in [9] to optimize the power levels of groups of users in the system. We modified the algorithm proposed in [5] and [6] to dynamically derive the optimal decoding schedule for the IMUD receiver. We investigated the complexity of the scheduling algorithm and proposed methods to reduce the complexity to be similar to the BCJR algorithm. We then showed through simulation that this power optimized system using dynamic scheduling achieves similar BER performance as a conventional receiver with significant complexity savings. Furthermore it outperforms the statically derived optimal schedule through reducing the variance of the per packet BER. We also proposed a method for estimating the SNR in an AWGN CDMA channel and showed that power and schedule may be optimized without any trade-off. Finally, we determined that a combination of static and dynamic scheduling offers the best benefit for the cost.

## References

[1] G. Caire, R. Müller, and T. Tanaka, "Iterative multiuser joint decoding: Optimal power allocation and low-complexity implementation," *IEEE Trans. Inform. Theory*, vol. 50, no. 9, pp. 1950–1973, Sept. 2004.

[2] C. Schlegel and Z. Shi, "Optimal power allocation and code selection in iterative detection of random CDMA," in *Proc. Zurich Seminar on Communications*, Zurich, Switzerland, Feb. 2004, pp. 98–101.

[3] R. Müller and G. Caire, "The optimal received power distribution for IC-based iterative multiuser joint decoders," in *Proc. Allerton Conf. on Commun., Control and Computing*, Monticello, USA, Oct. 2001.

[4] S. ten Brink, "Convergence behavior of iteratively decoded parallel concatenated codes," *IEEE Trans. Commun.*, vol. 49, no. 10, pp. 1727–1737, Oct. 2001.

[5] F. Brännström, L. K. Rasmussen, and A. J. Grant, "Convergence analysis and optimal scheduling for multiple concatenated codes," *IEEE Trans. Inform. Theory*, vol. 51, pp. 3354–3364, Sept. 2005.

[6] D. P. Shepherd, F. Brännström, and M. C. Reed, "Minimising complexity in iterative multiuser detection using dynamic decoding schedules," in *Proc. IEEE Int. Workshop on Sig. Proc. Advanced in Wireless Communications*, Cannes, France, 2006, pp. 1–5.

[7] K. Li and X. Wang, "EXIT chart analysis of turbo multiuser detection," *IEEE Trans. Wireless Commun.*, vol. 4, no. 1, pp. 300–311, Jan. 2005.

[8] J. W. Lee and R. E. Blahut, "Convergence analysis and BER performance of finite-length turbo codes," *IEEE Trans. Commun.*, vol. 55, no. 5, pp. 1033–1043, May 2007.
[9] D. P. Shepherd, F. Schreckenbach, and M. C. Reed, "Optimization of unequal power coded multiuser DS-CDMA using extrinsic information transfer charts," in *Proc. Conf. Info. Sciences and Systems*, Princeton, USA, Mar. 2006, pp. 1435–1439.
[10] D. Shepherd, F. Brännström, and M. Reed, "Dynamic scheduling for a turbo CDMA receiver using EXIT charts," in *Proc. Aust. Commun. Theory Workshop*, Adelaide, Australia, Feb. 2007, pp. 34–38.
[11] P. D. Alexander, A. J. Grant, and M. C. Reed, "Performance analysis of an iterative decoder for code-division multiple-access," *European Trans. Telecom.*, vol. 9, no. 5, pp. 419–426, Sept./Oct. 1998.
[12] "3GPP TS 25.104 V5.9.0; 3rd generation partnership project;technical specification group radio access network;base station (BS) radio transmission and reception (FDD) (release 5)," Sept. 2004.
[13] D. P. Shepherd, Z. Shi, M. Anderson, and M. C. Reed, "EXIT chart analysis of an iterative receiver with channel estimation," in *Proc. IEEE Global Telecommunications Conf.*, Washington D.C., USA, Nov. 2007, pp. 4010–4014.
[14] Z. Shi and C. Schlegel, "Performance analysis of iterative detection for unequal power coded CDMA systems," in *Proc. IEEE Global Telecommunications Conf.*, vol. 3, Dec. 2003, pp. 1537–1542.
[15] D. P. Shepherd, F. Brännström, and M. C. Reed, "Fidelity charts and stopping/termination criteria for iterative multiuser detection," in *Proc. 4th Int. Symp. on Turbo Codes and Related Topics*, Munich, Germany, 2006.
[16] F. Brännström and L. K. Rasmussen, "Non-data-aided parameter estimation in an additive white gaussian noise channel," in *Proc. IEEE Int. Symp. on Info. Theory*, Adelaide, Australia, 2005, pp. 1446–1450.
[17] F. Brännström, "Convergence analysis and design of multiple concatenated codes," Ph.D. dissertation, Chalmers University of Technology, Göteborg, Sweden, 2004.
[18] M. Tuchler and J. Hagenauer, "EXIT charts of irregular codes," in *Proc. Conf. Info. Sciences and Systems*, Princeton, USA Mar. 2002.
[19] F. Schreckenbach and G. Bauch, "Bit-interleaved coded irregular modulation," *European Trans. Telecommun.*, vol. 17, pp. 269–282, Mar. 2006.
[20] T. Coleman and Y. Li, "An interior, trust region approach for nonlinear minimization subject to bounds," *SIAM J. Optimization*, vol. 6, pp. 418–445, 1996.
[21] ——, "On the convergence of reflective newton methods for large-scale nonlinear minimization subject to bounds," *Mathematical Programming*, vol. 67, no. 2, pp. 189–224, 1996.
[22] V. Franz and J. B. Anderson, "Concatenated decoding with a reduced-search BCJR algorithm," *IEEE J. Select. Areas Commun.*, vol. 16, no. 2, pp. 186–195, Feb. 1998.
[23] U. Dasgupta and K. R. Narayanan, "Parallel decoding of turbo codes using soft output $T$-algorithms," *IEEE Commun. Lett.*, vol. 5, no. 8, pp. 352–354, Aug. 2001.

**David Shepherd** was born in Sydney, Australia, in December 1977. He was awarded a B.Eng. with Honours at the Australian National University in Canberra in 2003. He has been working towards the Ph.D. Degree at National ICT Australia since October 2004. Besides being an elite-level athlete who has represented Australia at several World Orienteering Championships, David has spent periods in 2005 and 2006 as a visiting researcher at the Department of Signals and Systems at Chalmers University of Technology in Göteborg, Sweden. His research interests include turbo receiver analysis and design and iterative channel estimation. David has published a number of conference papers and is listed as an author on one patent application. He is currently writing his Ph.D. thesis.

**Fredrik Brännström** was born on April 8, 1974, in Luleå, Sweden. He received the M.Sc. degree in Electrical Engineering from LuleåUniversity of Technology, Luleå, Sweden in 1998, the Lic.Eng. degree in Communication Theory and the Ph.D. degree in Communication Theory from the Department of Computer Engineering, Chalmers University of Technology, Göteborg, Sweden in 2000 and 2004, respectively. He has spent periods of 2001, 2002, 2003, and 2005 as a visiting researcher at the Institute for Telecommunications Research, University of South Australia, Australia. From 2004 to 2006, he had a Post Doc position in the Communication Systems Group at the Department of Signals and Systems, Chalmers University of Technology, Göteborg, Sweden. Dr. Brännström is currently with Quantenna Communications, Sunnyvale, California. His research interests include code design and efficient iterative processing.

**Frank Schreckenbach** received his Dipl.-Ing. and Dr.-Ing. degree in Electrical Engineering from Munich University of Technology (TUM), Germany, in 2001 and 2007, respectively. In 1999/2000, he studied at Virginia Polytechnic Institute and State University, USA. From 2001 to 2006 he was member of scientific staff at the Institute for Communications Engineering of the Munich University of Technology. In 2005, he was a visiting researcher at National Information and Communications Technology Australia (NICTA) in Canberra, Australia. In 2007, he joined the Institute of Communications and Navigation at the German Aerospace Center (DLR) where he is currently working in the area of aeronautical communications.

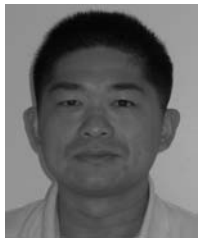

**Zhenning Shi** received his BS degree in Electronics Engineering from Tsinghua University, China, in 1998, and his PhD degree in Electrical and Computer Engineering from the University of Utah, US, in 2003. His doctoral research is on analysis and algorithm development for iterative multiuser receivers. From 2002 to 2004, he worked as a post-doctoral fellow at the Electrical and Computer Engineering Department, University of Utah, in collaboration with L-3 Communications on a project to develop low-complexity multiuser detection methods based on Monte-Carlo Markov Chain (MCMC). He is currently a research staff member at National ICT Australia, and is an adjunct research fellow at Australian National University (ANU). His recent work has been focused on signal processing techniques for OFDM-based systems.

Zhenning Shi's primary research interests include the Turbo receiver design, multiuser detection, synchronization, channel estimation and equalization in time-frequency selective channels, CDMA, MIMO, and OFDMA systems. He has published 40 journal and conference papers, and is listed as an author on four patent applications.

**Mark C. Reed** has worked in industry and research positions for the last 17 years with positions in the U.S.A., Switzerland, and Australia. He pioneered the area of iterative receiver design as part of his doctoral studies and was part of a team that designed and developed a world first Satellite-UMTS Modem for the European Space Agency. He also completed further work on 3G Basestation design as technical lead in the highly successful European Commission project, ASILUM, which investigated and validated advanced signal processing schemes for link improvement in UMTS. Since April 2003 Dr Reed is employed as a Principle Researcher at the National ICT Australia (NICTA), and is an Adjunct Assoc. Professor at the Australian National University, Canberra, Australia, where he is involved in research, education, and commercialization, in wireless signal processing. He has over 50 international journal and conference papers, he was an Associate Editor for the IEEE TRANSACTIONS ON VEHICULAR TECHNOLOGY (2005-2007), and has been listed as inventor on seven patent applications.